

1           **Increasing age is independently associated with higher free water in non-**  
2           **active MS brain - A multi-compartment analysis using FAST-T2**

3           Liangdong Zhou<sup>1,2</sup>, Yi Li<sup>1,2\*</sup>, Xiuyuan Wang<sup>1,2</sup>, Elizabeth Sweeney<sup>1</sup>, Hang Zhang<sup>1,4</sup>,  
4           Emily B. Tanzi<sup>1,2</sup>, Jennette Prince<sup>5</sup>, Victor Antonio Su-Ortiz<sup>5</sup>, Susan A. Gauthier<sup>3</sup>, Thanh D.  
5           Nguyen<sup>1,4\*</sup>

6           1, Radiology Department 2, Brain Health imaging Institute 3, Neurology Department 4, MRI  
7           Research Institute; Weill Medical College of Cornell University, New York, NY, United States 5,  
8           Department of Biomedical Engineering of Cornell University Ithaca, NY, United States

9           \* Corresponding authors:

10          Dr. Yi Li, [yil4008@med.cornell.edu](mailto:yil4008@med.cornell.edu), Dr. Thanh D. Nguyen, [tdn2001@med.cornell.edu](mailto:tdn2001@med.cornell.edu)

11          420 E 70st St, LH 400, New York, NY, 10021, United States

12

13          Wolds count: 3125

14

15

16

17

18

19

20

21

22

## 1        **Highlights**

- 2        • MR T2 relaxometry is a valid method to quantify the cerebrospinal fluid fraction  
3        (CSFF) in cerebral cortical regions
- 4        • The CSFF in the cerebral cortical regions are positively correlated with age by  
5        controlling the white matter lesion load in non-active MS subjects.
- 6        • Quantification of cerebral CSFF may reflect the perivascular space load in  
7        cortex and better interpret the disease progression in neurodegenerative disease,  
8        such as MS.

## 9        **Abstract**

### 10       **Purpose**

11        To explore the relationship between the cerebral cortical perivascular space (PVS)  
12        and aging in non-active MS subjects by using the multi-echo T2 relaxometry based  
13        cerebrospinal fluid fraction (CSFF) map.

### 14       **Methods**

15        Multi-echo spiral T2 data from 111 subjects with non-active multiple sclerosis  
16        (MS) were retrospectively investigated by fitting the T2 data into a three-compartment  
17        model, the three water compartments including myelin water, intra-extracellular water,  
18        and cerebrospinal fluid. Segmentation of T1w image was performed to get the region  
19        of interest (ROI) in cerebral cortical regions. The white matter lesion segmentation was  
20        conducted using a convolutional neural network (CNN) based segmentation tool. The  
21        CSFF in the ROIs were correlated with age by controlling the gender, white matter  
22        hyperintensity lesion burden, and MS disease duration. Multiple linear models were  
23        created for the analysis of aging effect on the CSFF.

1           **Results**

2           The ROI analysis shows that the CSFF in the cerebral cortical regions (temporal,  
3           occipital, parietal, front, hippo, and mtl) are significantly linear increasing with age  
4           ( $p<0.01$ ). The intra-extracellular water fraction (IEWF) in the ROIs are significantly  
5           linear decreasing ( $p<0.01$ ).

6           **Conclusion**

7           The multi-echo T2 based three-compartment model can be used to quantify the  
8           CSFF. The linear increase of CSF water contents in the cerebral cortical regions  
9           indicates increased perivascular space load in cortex with aging. The quantification of  
10          CSFF may provide a way to understand the glymphatic clearance function in aging and  
11          neurodegenerations.

12

13          **Keywords**

14          Cerebrospinal fluid water fraction (CSFF), water compartment modeling, multiple  
15          sclerosis, aging, brain clearance

16

17

18

19

20

21

22

23

24

## 1 1 Introduction

2 Dilated perivascular space (PVS) (1), or Virchow-Robin (VR) spaces, is common  
3 radiology finding in clinical practice and brain research. PVS surround the walls of  
4 vessels as they penetrate through the brain parenchyma from the subarachnoid space,  
5 which has been verified functioning as brain clearance pathway of the glymphatic  
6 system in recent studies (2–4). However, only enlarged PVS is visible in clinical MRI  
7 examination, and those along small vessels in cerebral cortex are hard to see in regular  
8 MRI sequence (5). There are studies on the scoring system for qualitative evaluating of  
9 the PVS (5). The qualitative scoring system categorize the subjects into 5 groups by  
10 counting the PVS number on the slice of semioval. This scoring system could be  
11 inaccurate due to the poor image quality, and the unequal distribution of the PVS across  
12 image slice. There are also quantitative method for evaluating the PVS volume (6–8).  
13 They are doing the imaging processing, such as image enhancement, segmentation,  
14 based on the multimodal MRI. Therefore, the performance of the methods also highly  
15 relies on the image quality. Most importantly, imaging processing-based methods have  
16 an inherent disadvantage for PVS evaluating, that is they are not able to handle the  
17 invisible PVS that are not shown in the image, no matter qualitative or quantitative  
18 methods. It has been shown that the CSF water accumulates in the PVS (9,10). This  
19 provides us an alternative way to measure the PVS by quantifying the CSF water. T2  
20 relaxometry based three water compartment model has been applied in brain research  
21 for quantitative water fraction measure, but all of them focused on the myelin water in  
22 multiple sclerosis (MS) study (11–13).

23 MS is a complex disease, characterized by inflammatory demyelination and axonal  
24 degeneration. It is hard to treat because the etiology is unknown. A better understanding  
25 of the disease mechanism will facilitate the development of new therapies (14). Aging  
26 is the most common cause of neurodegenerations. We utilized aging as a risk factor of  
27 neurodegenerations and tested its relationship with brain parenchyma CSF fraction  
28 (CSFF) in non-active MS brain. CSFF has been hypothesized as a potential biomarker

1 of perivascular space (PVS) of vessels, which has been verified functioning as brain  
2 clearance pathway of the glymphatic system in recent studies (2–4). We hypothesize  
3 that cerebral cortex CSFF will increase with aging in non-active MS independent of  
4 white matter lesion load (neuroinflammation). T2 relaxometry-based multiple water-  
5 compartment method has been applied in brain research for quantitative water fraction  
6 measure (15), but most of them focused on the myelin water in multiple sclerosis study  
7 (11–13). In this study, we first applied the spiral trajectory T2 relaxometry method  
8 described in (15) and the three-pool water compartment model (13) in cerebral cortical  
9 regions to quantify the CSF water fraction and investigated the aging effect on PVS.  
10 We hypothesize that this method will improve the capability of detecting the PVS  
11 change in aging and neurodegeneration disease.

## 12 2 Material and methods

### 13 2.1 Theory

14 The three water compartment model has been used in the myelin water  
15 quantification in the MS study (13,16,17). In this study we follow the similar procedure  
16 as in (13) for the quantification of CSF water. According to the T2 relaxation time  
17 difference, the brain water can be modeled as three compartments: the myelin water  
18 with T2 time about 10 ms, the intra-extracellular water with T2 time about 50-80 ms,  
19 and the CSF water or free water with T2 time larger than 1000 ms at 3T (18). Therefore,  
20 the measured MR signal  $S(t)$  in three-pool water compartment model can be written  
21 as

$$22 \quad S(TE) = A_{my}e^{-TE/T_{2,my}} + A_{ie}e^{-TE/T_{2,ie}} + A_{csf}e^{-TE/T_{2,csf}}, \quad [1]$$

23 where  $TE$  is the echo time,  $A_{my}$ ,  $A_{ie}$ , and  $A_{csf}$  are the signal amplitude attribute to  
24 the three water compartments,  $T_{2,my}$ ,  $T_{2,ie}$  and  $T_{2,csf}$  are the T2 time of the three  
25 water compartments, respectively.

1 The measured signal can then be fitted to the model [1] using nonlinear least square (16)  
 2 with multiple  $TE$ s to obtain the solution  $\mathbf{x} = (A_{my}, A_{ie}, A_{csf}, T_{2,my}, T_{2,ie}, T_{2,csf})$ :

$$3 \quad \mathbf{x} = \operatorname{argmin}_{\mathbf{x}} \sum_{n=1}^N \|S(\mathbf{x}, TE_n) - S_{measure}^n\|_2^2 + \lambda \|\nabla_s \mathbf{x}\|_2^2, \quad [2]$$

4 where  $S(\mathbf{x}, TE_n)$  is the signal model in [1] with  $n$ -th TE,  $N$  is the total number of  
 5 TE,  $S_{measure}^n$  is measured signal at  $TE_n$ ,  $\lambda$  is the regularization parameter to impose  
 6 a spatially local smoothness of the solution (19), and  $\nabla_s$  is the 2D discrete Laplace  
 7 operator. The regularization parameter was selected by testing on the healthy subjects  
 8 with various  $\lambda$  and chose the one that generated myelin water map with the best visual  
 9 quality.

10 Then the CSF water fraction (CSFF) map can be calculated as:

$$11 \quad CSFF = A_{csf} / (A_{my} + A_{ie} + A_{csf}) * 100. \quad [3]$$

## 12 2.2 Subjects

13 This was a retrospective study. 111 non-active MS patients (male: 33, female: 78,  
 14 age:  $58.02 \pm 9.70$  years, maximum age: 79, minimum age: 45) were scanned as part of  
 15 a large imaging research database for MS disease. The 111 subjects were filtered by  
 16 using the following three conditions to avoid the effect of progression of the disease on  
 17 our purpose:

- 18 1. MS is non-active,
- 19 2. Have diagnosis, MRI and clinic visits,
- 20 3. The gap of diagnosis and MRI visits is less than 12 months.

21 The details of the filtered subjects' information are listed in the Table 1.

	Female	Male	Total
<b>No. of subject</b>	78	33	111
<b>Age (SD)</b>	57.42 (9.47)	59.42 (10.22)	58.02 (9.70)
<b>DD (SD)</b>	17.56 (9.46)	17.91 (9.29)	17.66 (9.37)
<b>MSLB (SD)</b>	13.04 (15.04)	10.64 (15.42)	12.33 (15.12)

22 TABLE 1 BASIC INFORMATION OF THE SUBJECTS.

### 1 **2.3 Data acquisition**

2 Multi-echo T2 data was acquired with Fast Acquisition with Spiral Trajectory and  
3 adiabatic T2prep (FAST-T2) sequence at 3T. The FAST-T2 imaging parameters were  
4 as follows: axial field of view = 24 cm; matrix size =  $192 \times 192$  (interpolated to  $256 \times$   
5  $256$ ); slice thickness = 5 mm; number of slices = 32; spiral TR = 7.8 ms; spiral TE =  
6 0.5 ms; number of spiral leaves per stack = 32; flip angle =  $10^\circ$ ; readout bandwidth =  
7  $\pm 125$  kHz; TEs = 0, 7.6, 17.6, 67.6, 147.6, 307.6 ms. Corresponding T1w, T2w, and  
8 T2FLAIR were also acquired at the same session for the anatomical structure and  
9 disease diagnosis.

### 10 **2.4 Data processing**

11 CSFF map was computed from multi-echo T2 data acquired with Fast Acquisition  
12 with Spiral Trajectory and adiabatic T2prep (FAST-T2) sequence at 3T. A three-  
13 compartment nonlinear least squares fitting algorithm with spatial regularization was  
14 used to derive the water fraction maps, with the component with the longest T2 assigned  
15 to CSF.

16 FreeSurfer was used on T1w for the segmentation of brain ROIs: frontal lobe,  
17 temporal lobe, occipital lobe, parietal lobe, hippo, and medial temporal lobe. The ROIs  
18 then were coregistered to the CSFF space and visually checked by three experienced  
19 radiologists for the accuracy of coregistration. CSFF in the ROIs was extracted for all  
20 subjects.

21 MS lesion was segmented using in-house developed model based on convolutional  
22 neural network with information of T1w, T2w, and T2FLAIR images. The absolute MS  
23 lesion volume was extracted from the segmentation. The skull size scaling factor was  
24 processed using FSL toolbox. The MS lesion burden (MSLB) was then computed by  
25 multiplying absolute volume with the skull size scaling factor for each subject. The  
26 skull size scaling factor was used for the normalization of different head size of subjects.

1 Eighty subjects without obvious MS lesion in the brain centrum semiovale region  
2 (BCS) were selected for the PVS score test. Three experienced neuroimaging  
3 researchers rated the PVS score of BCS in T2w image individually and arrived at a  
4 consensus PVS rating score for each subject by using a published method (5): 0 (none),  
5 1 (1-10), 2 (11-20), 3 (21-40), 4 (>40). . The CSFF in the white matter of the same  
6 region was extracted.

7 The disease duration (DD) is defined as the time gap between MRI date and diagnosis  
8 date.

## 9 **2.5 Data analysis**

10 As our goal is to analyze the relationship between CSFF and age, we have to  
11 control the effect of other factors such as the gender, DD, and MSLB. We use  
12 multivariate linear regression model for the data analysis. CSFF is the output and age,  
13 gender, DD, MSLB are the inputs of the model. Variance inflation factor (VIF) was  
14 computed for all variables to make sure there is no collinearity between variables. It  
15 turned out that the VIF for all variables are close to 1, which indicates there is no  
16 collinearity between variables. The cross correlation of variables was calculated to  
17 check the interactive effects. The distribution of MSLB is nonGaussian so that we have  
18 used a log transform to obtain a nearly normal distributed MSLB. The following  
19 describe the model for the two considered outputs:

$$20 \quad CSFF \sim Age + Gender + DD + \log(MSLB) \quad [4]$$

21 IEWF was not analyzed separately because  $CSFF + IEWF + MWF = 1$  and MWF is  
22 very small compare with CSFF and IEWF. The trends of IEWF with age is opposite to  
23 CSFF.

24 For the relationship between WM CSFF and PVS score on the semiovale slice, we  
25 fitted an ANOVA model.



1 To see how the DD affects the CSFF within the non-active MS cohort, we filtered  
2 our subjects with two conditions: one is subjects age  $\geq 50$  years old, the other one is  
3 grouping the filtered subjects using the first condition into two groups (DD\_long and  
4 DD\_short) by DD. The cutoff DD between the two groups is the median of DD (15  
5 years), 41 subjects for each group.

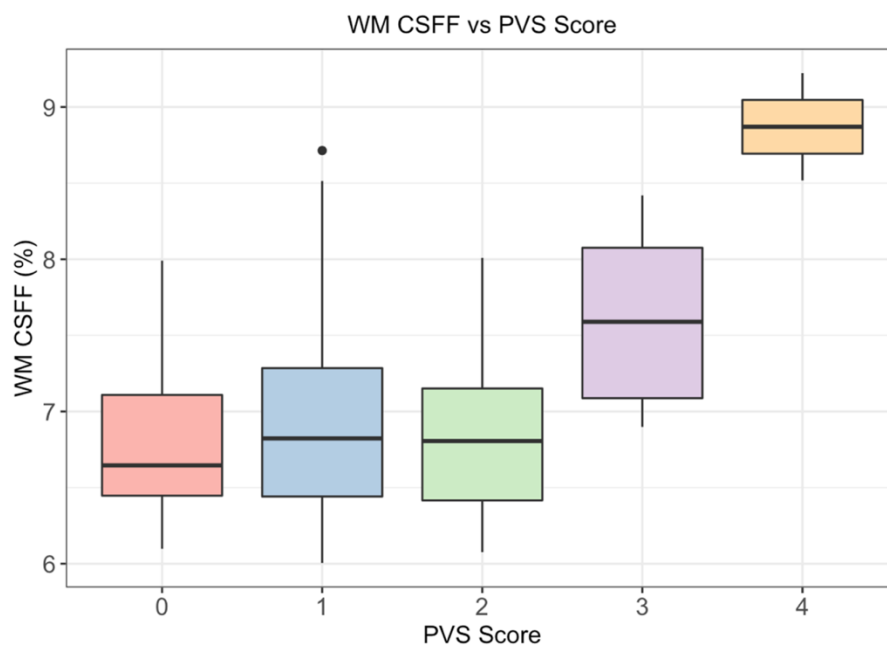
## 6 2.6 Code and data availability

7 The code and data are available with a request sending to the corresponding author  
8 by following the data sharing restrictions in our institute.

## 9 3 Results

### 10 3.1 CSFF with PVS score

11 We fit an ANOVA model and found that there was a difference in WM CSFF by  
12 PVS score ( $F = 5.83$ ,  $p$ -value  $< 0.001$ ), (Figure 1). This implies that CSFF can serve as  
13 an alternative indicator of PVS change. Interestingly, CSFF doesn't seem very different  
14 for PVS score 0-2, but starts to increase at a score of 3. The higher data variability of  
15 CSFF in groups 1 and 2 were observed.

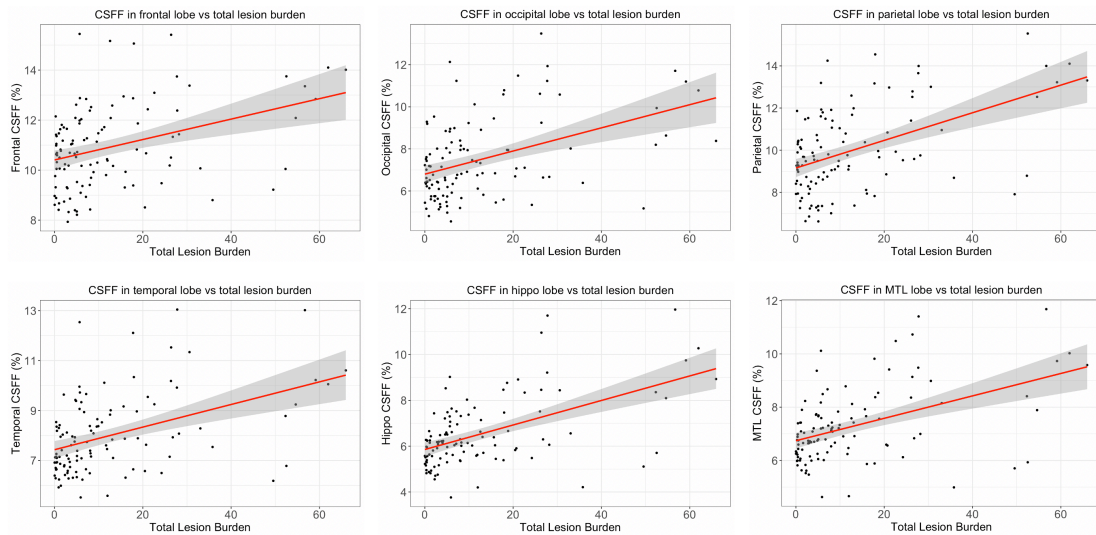


16

17 FIGURE 1 WM CSFF AND PVS SCORE OF CENTRUM SEMIOVALE WHITE MATTER.

## 1 3.2 CSFF with MSLB in WM

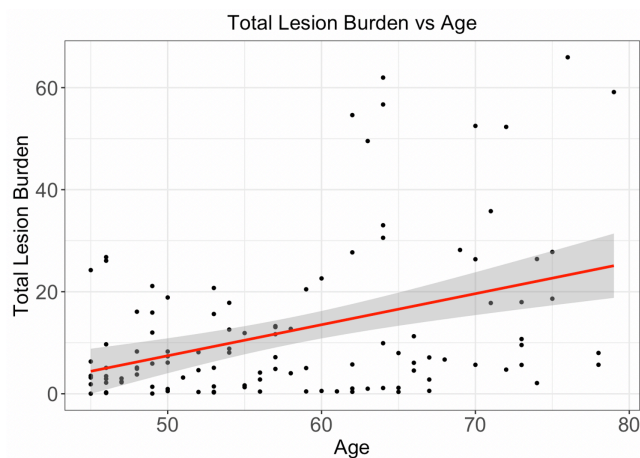
2 According to multiple simple linear regression analysis, it shows in Figure 2 that  
3 CSFF in all selected brain regions are significantly ( $p < 0.5$ ) linear with the total white  
4 matter lesion burden.



5  
6 FIGURE 2 CSFF VERSUS WHITE MATTER LESION BURDEN IN SELECTED BRAIN REGIONS. IT SHOWS  
7 THAT CSFF IS LINEAR WITH WM LESION BURDEN IN ALL SELECTED REGIONS WITH  $p < 0.01$ .

## 9 3.3 White matter lesion with age

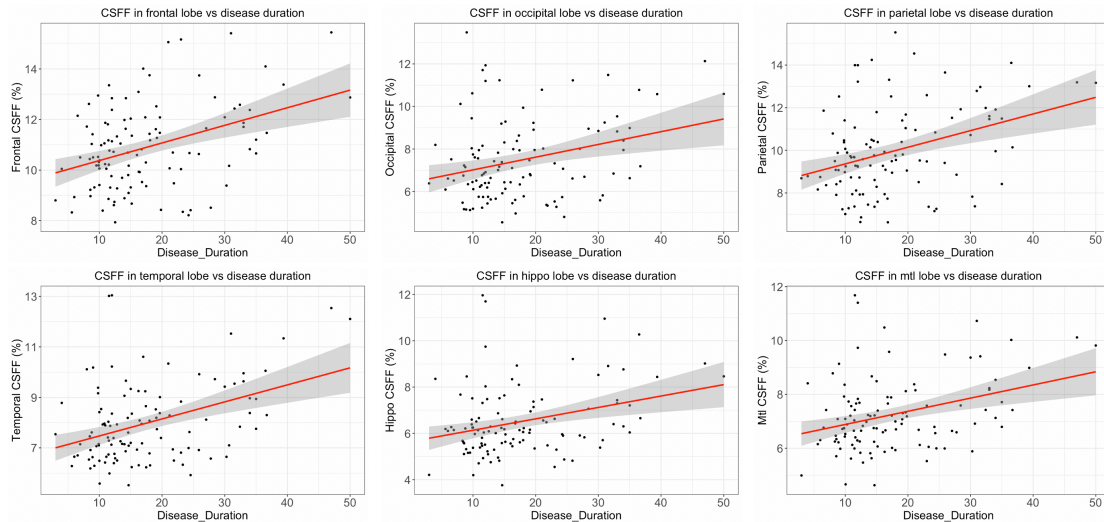
10 The linear relationship between the total white matter lesion burden and age is  
11 shown in Figure 3. This results is previously observed in literature (20,21).



12  
13 FIGURE 3 WHITE MATTER LESION BURDEN WITH AGE. IT SHOWS THAT THE WM LESION BURDEN IS  
14 LINEARLY CORRELATED WITH AGE ( $p < 0.01$ ).

### 1 3.4 CSFF with disease duration

2 The relations between CSFF and disease duration is presented in Figure 4. It shows  
3 the significant linear relationship between these two values.



4  
5 FIGURE 4 CSFF WITH DISEASE DURATION. IT SHOWS THAT CSFF IS SIGNIFICANTLY LINEAR WITH THE  
6 DISEASE DURATION IN ALL THE SELECTED BRAIN REGIONS ( $P < 0.01$ ).

### 7 3.5 CSFF with multiple variates analysis

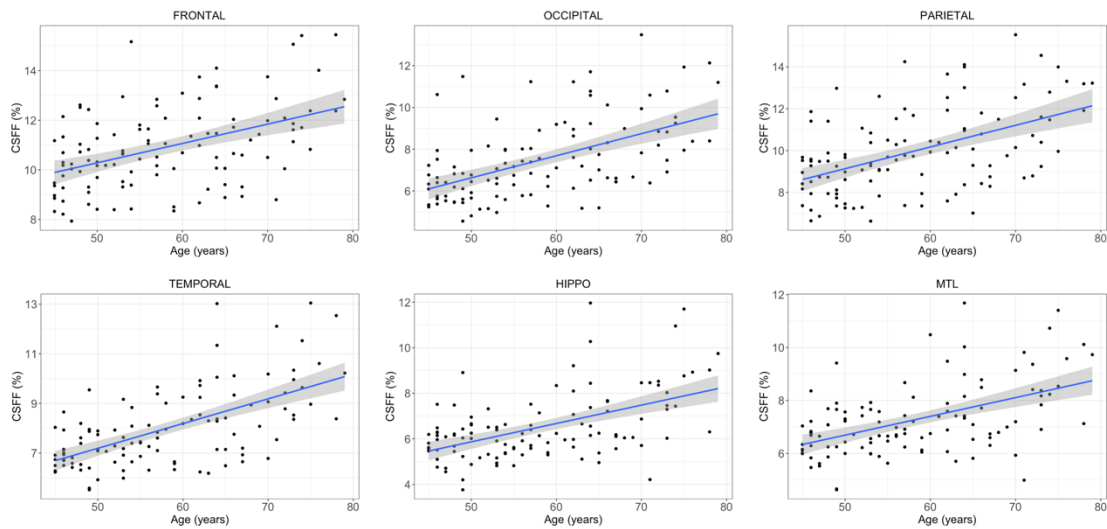
8 The VIF for variables are presented in Table 2. It shows that the VIF for all  
9 considered variables are close to 1, which is an indicator of absence of collinearity.  
10 Therefore, we can safely build a linear model to investigate the factors that have an  
11 effect on the output variables, CSFF, IEWF.

VIF table for variables				
Variables	Age	Gender	DD	MSLB
VIF	1.2606	1.0288	1.1317	1.1656

12 TABLE 2 VIF TABLE FOR VARIABLES TO DETERMINE IF THERE IS A COLLINEARITY BETWEEN VARIABLES.

13 The results in Figure 5 show that cerebral cortical CSFF significantly correlated  
14 with age in all brain lobes after controlling for gender, and for disease factors such as  
15 DD and MSLB. Table 3 shows the linear regression coefficients. The p-values in the  
16 last column indicates that all the variables have significant contribution to the output  
17 CSFF in the temporal lobe. We need to control the variables to extract the pure effects  
18 of variable on the output, i.e., we need to do the p-value adjustment by controlling the

1 variables. The p-value adjustment was done by utilizing the false discovery rate (FDR).  
 2 The FDR adjusted p-value for temporal CSFF regression model was shown in Table 4.  
 3 The regression model coefficients and the FDR adjusted p-value table for CSFF in other  
 4 ROIs similar to Table 3 and Table 4 can be found in the supplementary document.



5

6 FIGURE 5 LINEAR RELATIONSHIP BETWEEN CSFF AND AGE IN THE SIX REGIONS.

***Temporal CSFF ~ Age + Gender + DD + log (MSLB)***

	Estimate	Std. Error	t value	p value
<b>(Intercept)</b>	2.3286	0.6513	3.576	5.28e-4 ***
<b>Age</b>	0.0699	0.0124	5.625	1.52e-7 ***
<b>GenderM</b>	0.635	0.2370	2.679	0.0086 **
<b>DD</b>	0.0338	0.0122	2.775	0.0065 **
<b>log(MSLB)</b>	0.4074	0.1046	3.894	1.73e-4 ***

Significant codes: 0:\*\*\* 0.001:\*\* 0.01:\* 0.05:.

7 TABLE 3 MULTIVARIABLE ANALYSIS OF CSFF IN TEMPORAL LOBE WITH AGE, GENDER, DD, AND  
 8 MSLB.

<b><i>Temporal CSFF</i></b>	<b>FDR adjusted p-value</b>	<b>FDR significance</b>
<b>(Intercept)</b>	0.0021116	TRUE
<b>Age</b>	0.0000018	TRUE
<b>GenderM</b>	0.0205367	TRUE
<b>DD</b>	0.0195796	TRUE

MSLB

0.0010378

TRUE

TABLE 4 FDR ADJUSTED P-VALUE FOR TEMPORAL CSFF REGRESSION MODEL.

### 3.6 CSFF for subjects with long disease duration

Figure 6 presents the boxplots of the two group subjects in CSFF, age, DD, and MSLB. It shows that there is no significant age and MSLB difference between two groups. However, we observe significant difference of CSFF between two groups in the global gray matter, frontal and parietal lobes. And CSFF is marginally different in white matter for two groups.

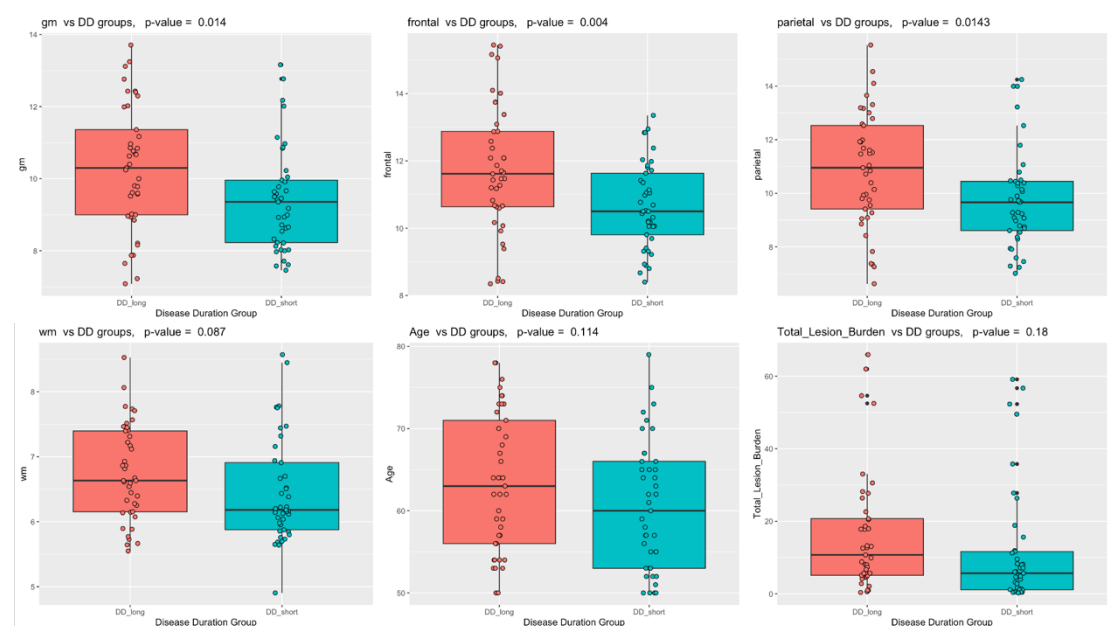


FIGURE 6 BOXPLOT OF THE CSFF, AGE, DD AND MSLB OF TWO GROUPS. IT SHOWS THAT CSFF FOR TWO GROUPS ARE SIGNIFICANTLY DIFFERENT IN GLOBE GRAY MATTER, FRONTAL LOBE, AND PARIETAL LOBE, BUT MARGINALLY SIGNIFICANTLY DIFFERENT IN GLOBAL WHITE MATTER.

## 4 Discussion

The role of neurodegeneration in MS has got more attention in recent years, which may involve the dysfunction of the recent discovered brain glymphatic system (22). PVS is an important pathway of the glymphatic system and has been reported link with aging and neurodegeneration disease. On the other hand, CSFF reflects the nature of CSF water compartment in brain parenchyma and has been hypothesized as a quantitative measure of PVS which was filled with CSF (9,10). T2 relaxometry based

1 modeling provides us an alternative way to measure PVS by evaluating the CSFF. With  
2 this method, we observed CSFF increases with aging in cerebral cortex for the first time  
3 by controlling MS disease factors, which indicates that CSFF could be a potential  
4 biomarker to evaluate PVS function in MS, which is an important pathway of  
5 glymphatic clearance.

6 MRI visible PVSs have been reported to increase with age in both WM and  
7 basal ganglia (23,24). This phenomenon has been long suspected in the  
8 cerebral cortex (25,26), but no human study has been reported because of a  
9 lack of a valid imaging tool. The quantification of CSFF not only includes the visible  
10 PVS shown in conventional MR image but also the invisible PVS in conventional MR  
11 image based on nature of the MR T2 relaxometry method.

12 We observed a linear increase of CSFF in cerebral cortex with age after controlling  
13 for disease duration and total white matter lesion burden. The diameter of large PVS  
14 (>3mm) increasing with age has been observed in the basal ganglia and white matter.  
15 We for the first time applied the multi-echo spiral T2 to map the CSF water fraction in  
16 cerebral cortex and observed CSF water compartment increased with aging in cerebral  
17 cortex in stable MS subjects. The proposed CSFF mapping method solves the problem  
18 of invisible PVS quantification in conventional PVS score system and potentially  
19 serves as a more accurate PVS quantification method. Glymphatic clearance play a  
20 important role is neurodegeneration disease such as AD, However, we need better  
21 understand it's role in MS.

22 In Figure 1, the PVS score increasing with age has been observed in the brain  
23 centrum semiovale region, which agrees with previous report. The CSFF doesn't seem  
24 very different for PVS score 0-2 but starts to increase at a score of 3. This may be  
25 because the portion of the visible enlarged PVS is a relatively small part of total PVS  
26 in those subjects, and the CSFF measure reflecting total PVS was driven by those

1 invisible small ones. The higher data variability of CSFF in groups 1 and 2 also  
2 indicates that varying levels of PVS were included in those groups.

3 The proposed CSFF quantification method has several advantages and potential  
4 applications. First, it is a biophysical based modeling fitting. This is the essential  
5 difference between our proposed method and the conventional image based  
6 postprocessing. Therefore, the CSFF method is not only able to quantify the free water  
7 in the visible PVS from MRI, but also capable of quantifying the free water in the PVS  
8 that surround the small vessels and invisible in the MRI. Second, to the best of our  
9 knowledge, this is the first study that quantify the CSFF in the cerebral cortex regions.  
10 Because the PVS in the cortex region usually presents as tiny or invisible dots on  
11 conventional MRI, this approach offers a new way to investigate the PVS load in brain  
12 parenchyma.

13 Moreover, the accurate PVS quantification from CSFF is promising to be applied  
14 in the neurodegenerative disease. The CSF is found playing the key role in the waste  
15 clearance procedure. An accurate CSF quantification in brain parenchyma might open  
16 a door for the mystery of many diseases, such as MS, AD, PD, SVD. For instance, in  
17 this study, we found that in elderly subgroup of the non-active MS subjects, the CSFF  
18 increase significantly in the frontal and parietal lobes for those subjects with long  
19 disease duration but without significant age difference between two groups as shown  
20 in Figure 6. This could imply that MS disease of long duration keep affecting the brain  
21 in a subtle way, which could be monitored by the quantification of CSFF.

22 Besides the advantages mentioned above, there are several limitations of this study.  
23 First, the data is limited. More data with various type of MS disease could be helpful to  
24 explore the behavior of CSFF in a broad perspective. Second, the CSFF could be a  
25 biomarker of PVS. However, this hypothesis is not fully validated. We scored the PVS  
26 number by visual check of T2w image, which could be biased by image resolution and  
27 radiologist experiences. Theoretically, CSFF represents the free water fraction which

1 includes free water in visible PVS and invisible PVS in T2w image. It is our future  
2 work to validate the relation between CSFF and PVS using postmortem study.

### 3 5 Conclusions

4 We proposed a T2 relaxometry based CSFF quantification method, which is able  
5 to quantify the CSF water in brain parenchyma. Analysis shows that the CSFF  
6 correlates with PVS score. The linear increase of CSF water contents in the cerebral  
7 cortical regions indicates the increased perivascular space load in cortex with aging.  
8 The quantification of CSFF could potentially provide a way to understand the PVS  
9 function in brain aging and neurodegenerations, which is part of the glymphatic  
10 clearance system.

11

### 12 Acknowledgement

13 Supported by NIH grants: AG057848.

### 14 Reference

- 15 1. Kwee RM, Kwee TC. Virchow-Robin Spaces at MR Imaging. *RadioGraphics*  
16 2007;27:1071–1086 doi: 10.1148/rg.274065722.
- 17 2. Brown R, Benveniste H, Black SE, et al. Understanding the role of the perivascular  
18 space in cerebral small vessel disease. *Cardiovasc. Res.* 2018;114:1462–1473 doi:  
19 10.1093/cvr/cvy113.
- 20 3. Durcanova B, Appleton J, Gurijala N, et al. The Configuration of the Perivascular  
21 System Transporting Macromolecules in the CNS. *Front. Neurosci.* 2019;13 doi:  
22 10.3389/fnins.2019.00511.
- 23 4. Zhu Yi-Cheng, Tzourio Christophe, Soumaré Aïcha, Mazoyer Bernard, Dufouil  
24 Carole, Chabriat Hugues. Severity of Dilated Virchow-Robin Spaces Is Associated  
25 With Age, Blood Pressure, and MRI Markers of Small Vessel Disease. *Stroke*  
26 2010;41:2483–2490 doi: 10.1161/STROKEAHA.110.591586.
- 27 5. Potter GM, Chappell FM, Morris Z, Wardlaw JM. Cerebral Perivascular Spaces  
28 Visible on Magnetic Resonance Imaging: Development of a Qualitative Rating Scale  
29 and its Observer Reliability. *Cerebrovasc. Dis. Basel Switz.* 2015;39:224–231 doi:  
30 10.1159/000375153.



- 1 6. Ballerini L, McGrory S, Valdés Hernández M del C, et al. Quantitative measurements  
2 of enlarged perivascular spaces in the brain are associated with retinal microvascular  
3 parameters in older community-dwelling subjects. *Cereb. Circ. - Cogn. Behav.*  
4 2020;1:100002 doi: 10.1016/j.cccb.2020.100002.
- 5 7. Niazi M, Karaman M, Das S, Zhou XJ, Yushkevich P, Cai K. Quantitative MRI of  
6 perivascular spaces (PVS) at 3 Tesla for early diagnosis of mild cognitive impairment  
7 (MCI). *AJNR Am. J. Neuroradiol.* 2018;39:1622–1628 doi: 10.3174/ajnr.A5734.
- 8 8. Sepehrband F, Barisano G, Sheikh-Bahaei N, et al. Image processing approaches to  
9 enhance perivascular space visibility and quantification using MRI. *Sci. Rep.*  
10 2019;9:12351 doi: 10.1038/s41598-019-48910-x.
- 11 9. Mestre H, Kostrikov S, Mehta RI, Nedergaard M. Perivascular Spaces, Glymphatic  
12 Dysfunction, and Small Vessel Disease. *Clin. Sci. Lond. Engl.* 1979 2017;131:2257–  
13 2274 doi: 10.1042/CS20160381.
- 14 10. Bakker ENTP, Bacskai BJ, Arbel-Ornath M, et al. Lymphatic Clearance of the  
15 Brain: Perivascular, Paravascular and Significance for Neurodegenerative Diseases.  
16 *Cell. Mol. Neurobiol.* 2016;36:181–194 doi: 10.1007/s10571-015-0273-8.
- 17 11. Kwon OI, Woo EJ, Du YP, Hwang D. A tissue-relaxation-dependent neighboring  
18 method for robust mapping of the myelin water fraction. *NeuroImage* 2013;74:12–21  
19 doi: 10.1016/j.neuroimage.2013.01.064.
- 20 12. Kulikova S, Hertz-Pannier L, Dehaene-Lambertz G, Poupon C, Dubois J. A New  
21 Strategy for Fast MRI-Based Quantification of the Myelin Water Fraction: Application  
22 to Brain Imaging in Infants. *PLOS ONE* 2016;11:e0163143 doi:  
23 10.1371/journal.pone.0163143.
- 24 13. Nguyen TD, Deh K, Monohan E, et al. Feasibility and reproducibility of whole  
25 brain myelin water mapping in 4 minutes using fast acquisition with spiral trajectory  
26 and adiabatic T2prep (FAST-T2) at 3T: Whole Brain Myelin Water Mapping with  
27 FAST-T2. *Magn. Reson. Med.* 2016;76:456–465 doi: 10.1002/mrm.25877.
- 28 14. Bjelobaba I, Savic D, Lavrnja I. Multiple Sclerosis and Neuroinflammation: The  
29 Overview of Current and Prospective Therapies. *Curr. Pharm. Des.* 2017;23:693–730  
30 doi: 10.2174/1381612822666161214153108.
- 31 15. Nguyen TD, Wisnieff C, Cooper MA, et al. T2prep three-dimensional spiral  
32 imaging with efficient whole brain coverage for myelin water quantification at 1.5 tesla.  
33 *Magn. Reson. Med.* 2012;67:614–621 doi: 10.1002/mrm.24128.

- 1 16. Du YP, Chu R, Hwang D, et al. Fast multislice mapping of the myelin water fraction  
2 using multicompartment analysis of T decay at 3T: A preliminary postmortem study.  
3 *Magn. Reson. Med.* 2007;58:865–870 doi: 10.1002/mrm.21409.
- 4 17. Andrews T, Lancaster JL, Dodd SJ, Contreras-Sesvold C, Fox PT. Testing the three-  
5 pool white matter model adapted for use with T2 relaxometry. *Magn. Reson. Med.*  
6 2005;54:449–454 doi: 10.1002/mrm.20599.
- 7 18. Deoni SCL, Rutt BK, Arun T, Pierpaoli C, Jones DK. Gleaning multicomponent T1  
8 and T2 information from steady-state imaging data. *Magn. Reson. Med.* 2008;60:1372–  
9 1387 doi: 10.1002/mrm.21704.
- 10 19. Kumar D, Nguyen TD, Gauthier SA, Raj A. Bayesian algorithm using spatial priors  
11 for multiexponential T2 relaxometry from multiecho spin echo MRI. *Magn. Reson.*  
12 *Med.* 2012;68:1536–1543 doi: 10.1002/mrm.24170.
- 13 20. Nyquist PA, Bilgel M, Gottesman R, et al. Age Differences in Periventricular and  
14 Deep White Matter Lesions. *Neurobiol. Aging* 2015;36:1653–1658 doi:  
15 10.1016/j.neurobiolaging.2015.01.005.
- 16 21. Leeuw F-E de, Groot JC de, Achten E, et al. Prevalence of cerebral white matter  
17 lesions in elderly people: a population based magnetic resonance imaging study. The  
18 Rotterdam Scan Study. *J. Neurol. Neurosurg. Psychiatry* 2001;70:9–14 doi:  
19 10.1136/jnnp.70.1.9.
- 20 22. Nedergaard M, Goldman SA. Glymphatic failure as a final common pathway to  
21 dementia. *Science* 2020;370:50–56 doi: 10.1126/science.abb8739.
- 22 23. Banerjee G, Kim HJ, Fox Z, et al. MRI-visible perivascular space location is  
23 associated with Alzheimer’s disease independently of amyloid burden. *Brain J. Neurol.*  
24 2017;140:1107–1116 doi: 10.1093/brain/awx003.
- 25 24. Park M, Kim JW, Ahn SJ, Cha YJ, Suh SH. Aging Is Positively Associated with  
26 Peri-Sinus Lymphatic Space Volume: Assessment Using 3T Black-Blood MRI. *J. Clin.*  
27 *Med.* 2020;9 doi: 10.3390/jcm9103353.
- 28 25. Kress BT, Iliff JJ, Xia M, et al. Impairment of paravascular clearance pathways in  
29 the aging brain. *Ann. Neurol.* 2014;76:845–861 doi: 10.1002/ana.24271.
- 30 26. Morris AWJ, Carare RO, Schreiber S, Hawkes CA. The Cerebrovascular Basement  
31 Membrane: Role in the Clearance of  $\beta$ -amyloid and Cerebral Amyloid Angiopathy.  
32 *Front. Aging Neurosci.* 2014;6 doi: 10.3389/fnagi.2014.00251.

33